

Shuttle Radiation Dose Measurements in the International Space Station Orbits

Author(s): Gautam D. Badhwar

Source: Radiation Research, 157(1):69-75.

Published By: Radiation Research Society

DOI: [http://dx.doi.org/10.1667/0033-7587\(2002\)157\[0069:SRDMIT\]2.0.CO;2](http://dx.doi.org/10.1667/0033-7587(2002)157[0069:SRDMIT]2.0.CO;2)

URL: <http://www.bioone.org/doi/full/10.1667/0033-7587%282002%29157%5B0069%3ASRDMIT%5D2.0.CO%3B2>

BioOne (www.bioone.org) is a nonprofit, online aggregation of core research in the biological, ecological, and environmental sciences. BioOne provides a sustainable online platform for over 170 journals and books published by nonprofit societies, associations, museums, institutions, and presses.

Your use of this PDF, the BioOne Web site, and all posted and associated content indicates your acceptance of BioOne's Terms of Use, available at www.bioone.org/page/terms_of_use.

Usage of BioOne content is strictly limited to personal, educational, and non-commercial use. Commercial inquiries or rights and permissions requests should be directed to the individual publisher as copyright holder.

Shuttle Radiation Dose Measurements in the International Space Station Orbits¹

Gautam D. Badhwar²

NASA Johnson Space Center, Houston, Texas 77058-3696

Badhwar, G. D. Shuttle Radiation Dose Measurements in the International Space Station Orbits. *Radiat. Res.* 157, 69–75 (2002).

The International Space Station (ISS) is now a reality with the start of a permanent human presence on board. Radiation presents a serious risk to the health and safety of the astronauts, and there is a clear requirement for estimating their exposures prior to and after flights. Predictions of the dose rate at times other than solar minimum or solar maximum have not been possible, because there has been no method to calculate the trapped-particle spectrum at intermediate times. Over the last few years, a tissue-equivalent proportional counter (TEPC) has been flown at a fixed mid-deck location on board the Space Shuttle in 51.65° inclination flights. These flights have provided data that cover the expected changes in the dose rates due to changes in altitude and changes in solar activity from the solar minimum to the solar maximum of the current 23rd solar cycle. Based on these data, a simple function of the solar deceleration potential has been derived that can be used to predict the galactic cosmic radiation (GCR) dose rates to within $\pm 10\%$. For altitudes to be covered by the ISS, the dose rate due to the trapped particles is found to be a power-law function, $\rho^{-2/3}$, of the atmospheric density, ρ . This relationship can be used to predict trapped dose rates inside these spacecraft to $\pm 10\%$ throughout the solar cycle. Thus, given the shielding distribution for a location inside the Space Shuttle or inside an ISS module, this approach can be used to predict the combined GCR + trapped dose rate to better than $\pm 15\%$ for quiet solar conditions. © 2002 by Radiation Research Society

Society

INTRODUCTION

Space radiation presents an increased risk to the health and safety of astronauts. The International Space Station (ISS) flies in a 51.65° Mir inclination orbit with a restricted altitude range. An important aspect of radiation risk assessment is the ability to predict, monitor and potentially reduce astronaut exposures. The orbital station Mir provid-

ed nearly 13 years of continuous observations of radiation (1). Extensive time-resolved data were acquired during the seven NASA-Mir missions around the time of the solar minimum (2). Although a considerable volume of dose and dose-equivalent rate data have been acquired on both the Space Shuttle and the Mir station, predicting these rates using the trapped-belt models has been not been possible, because the models describe the energy spectrum at solar minimum and solar maximum conditions only. In an earlier study using dose-rate measurements made with thermoluminescent dosimeters on board the Shuttle from 1981 to 1998, it was shown (3) that the dose rate from trapped-belt particles was correlated with the atmospheric density. Empirical fits to the data were used to predict the dose rates at six different shielding locations in 28.5° and 57° inclination orbits, and to predict astronaut doses that were within $\pm 30\%$ of the measured values. Tissue-equivalent proportional counter (TEPC) data from the Mir orbital station (4) also showed that the trapped-particle dose rate was a power-law function of the atmospheric density. Although there were very few data at a Shuttle inclination of 51.65°, and the Mir data covered only about half of a solar cycle, these data showed the potential of using the atmospheric density as the driver for predicting dose rate inside the 58 modules accurately.

A 0.7-cm \times 0.7-cm right circular cylindrical TEPC simulating a 2- μ m-diameter tissue has been flown on more than 25 Space Shuttle flights, including eight flights in the ISS inclination orbit. Details of this instrument and its calibration were given by Badhwar *et al.* (5). Data acquired from these flights span the solar minimum to the solar maximum of the 23rd solar cycle and cover the expected altitude range.

This paper presents data from the eight 51.65° inclination Shuttle flights. These data show that a power law in atmospheric density describes the trapped-belt dose rates in the ISS orbit very well. The results show the potential to estimate radiation exposures accurately at locations on board the ISS during any period.

RESULTS

The Space Shuttle TEPC was flown on six flights in the mid-deck M5005 location of the Space Shuttle and for two

¹ Correspondence should be addressed to: F. A. Cucinotta, NASA Johnson Space Center, Radiation Health Office, Mail Code SA2, Houston, TX 77058; e-mail: francis.a.cucinotta@jsc.nasa.gov.

² Deceased August 28, 2001.

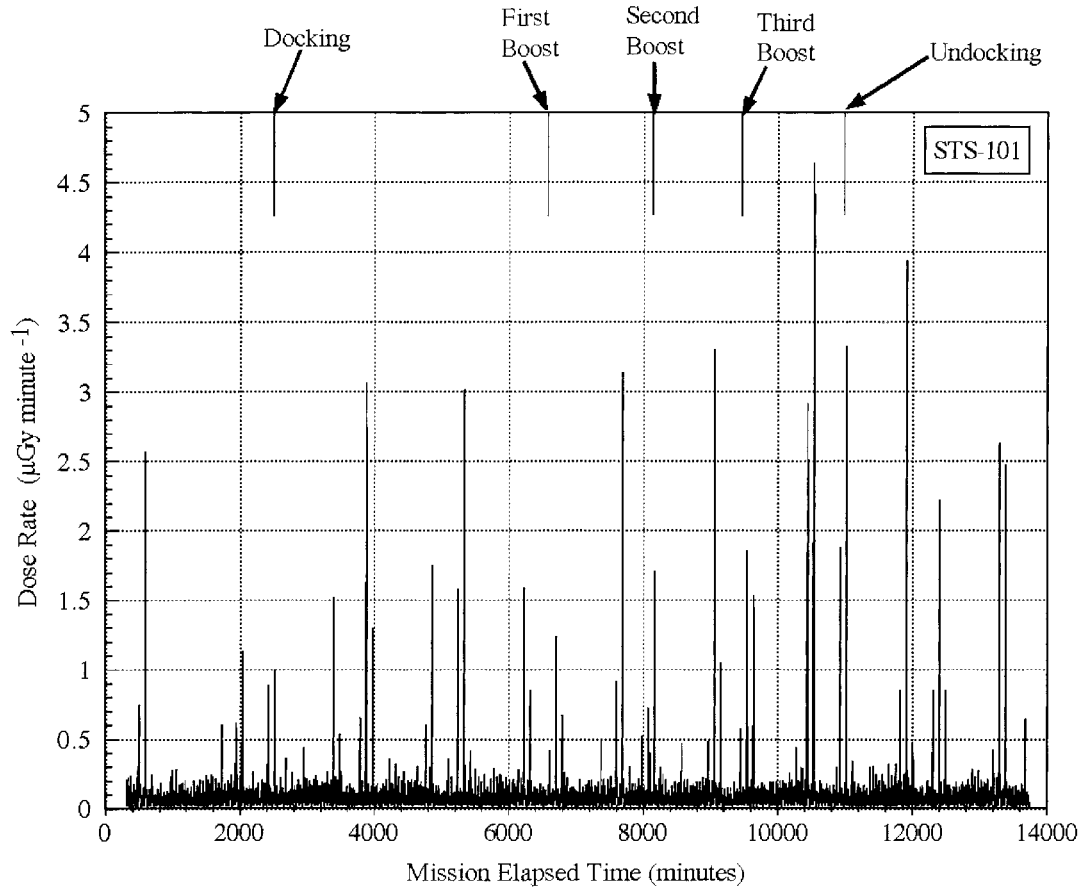


FIG. 1. A plot of measured dose rate as a function of the mission elapsed time for Space Shuttle flight STS-101.

flights near the sleeping station. Figure 1 plots the absorbed dose rate from Shuttle flight STS-101 as a function of the mission elapsed time. The sharp lines are from passage of the Shuttle through the South Atlantic anomaly (SAA), and the sinusoidal variation is due to the variation in the galactic cosmic radiation (GCR) dose rate with magnetic latitude. The data are easily separated into the SAA and the GCR components. There were small altitude boosts to the ISS orbit after the Shuttle docked with the station. The peak dose rate during the first set of SAA passes was about $2.5 \mu\text{Gy min}^{-1}$ prior to the docking of the Shuttle with the station. The dose rate decreased prior to the docking but increased after the docking. Obviously this change in rate cannot be due to the change in the effective shielding when the two spacecraft docked. The ratio of the average trapped dose rate for the Shuttle crossing the SAA to the trapped dose rate during the docking period was found to be 1.5, and it is attributed to the well-known east-west asymmetry of trapped-proton fluxes and asymmetry in the Shuttle shielding distributions. It arises because protons gyrating along the Earth's magnetic-field line that come from above the point of detection and those from below the point of detection traverse different path lengths of the atmosphere. This effect was clearly demonstrated on earlier Shuttle

flights (6, 7) on STS-31, -60 and -94, which led to the ratio of these dose rates of 1.63.

Table 1 summarizes the TEPC and TLD-100 measured dose rates and the solar conditions for each flight. The solar 10.7-cm radio flux is directly proportional to its UV output, which drives the changes in the atmospheric density, and hence the trapped-proton fluxes. The solar deceleration potential is a measure of the average energy loss ($Ze\phi$, where Ze is the charge) suffered by a GCR particle as it moves against the outward-flowing solar wind from the local interstellar medium to the point of observation inside the heliosphere. It controls the spectrum of GCR particles (8). The TEPC on STS-63 and -71 was located at the less shielded Dloc2 location. The STS-63 trapped-particle dose rate and the particle fluxes were scaled down to correspond to the MS005 shielding distribution. The scaling factor, 2.015, was derived using the solar minimum orbit-averaged trapped-particle model flux and the Shuttle + TEPC detector shielding distribution functions at the two locations. Because of a single-event induced error, the STS-71 TEPC operated for just 12 h, and no useful data on trapped particles could be extracted. Thus the data in Table 1 correspond to the MS005 mid-deck shielding location. The TLD-100 measurement errors are about 1% and, based on

TABLE 1
Absorbed Dose and Dose-Equivalent Rates for 51.65° Inclination Shuttle Flights

Mission	Launch date	Mission duration (days)	Dose rate ($\mu\text{Gy/day}$)		Dose-equivalent rate ($\mu\text{Sv/day}$)		Altitude (km)	F10.7 (10^4 Jansky)	Deceleration potential (ϕ , MV)	Total dose rate ($\mu\text{Gy/day}$)	Average crew dose rate (TLD-100) ($\mu\text{Gy/day}$)
			GCR	Trapped	GCR	Trapped					
STS-63	2/3/1995	8.27	109.8	153.1	386.4	269.5	373	81	559	262.9	273.3
STS-71	6/27/1995	9.81	132.8	—	404.7	—	295	81	551	—	284.5
STS-88	12/4/1998	11.80	120.2	142.5	518.0	255.8	320	142	608	262.7	209.1
STS-91	6/2/1998	9.83	145.4	102.6	551.8	203.1	368	116	467	248.0	225.9
STS-96	5/27/1999	9.80	118.9	72.6	515.0	137.5	320	169	682	191.5	206.1
STS-101	5/19/2000	9.86	106.2	34.6	301.9	62.2	343	200	875	140.8	117.9
STS-106	9/8/2000	11.80	112.3	66.8	333.9	122.4	328	167	1051	179.1	148.4
STS-92	10/11/2000	12.90	102.9	63.0	436.3	114.1	328	158	1127	165.9	155.9

their calibration using heavy-ion accelerators, they may underestimate the dose by 5–10% because of their decreased efficiency for particles with high linear energy transfer.

Figure 2 plots the average (typically six astronauts on each flight) astronaut TLD-100 measured total absorbed dose rate, $D_{\text{Astronaut}}$, as a function of the TEPC total dose rate, D_{TEPC} . The solid line is the weighted least-squares fit: $D_{\text{Astronaut}} = -(5.2 \pm 32.3) + (0.91 \pm 0.18) D_{\text{TEPC}}$. Unlike the TLD-100, the TEPC, is far more sensitive to secondary neutrons, leading to a small increase in the TEPC absorbed dose rate. The fitted line shows that the TEPC measurement is an excellent representation of the average Shuttle astronaut absorbed dose rate. It varied from about 120 μGy

day^{-1} to about 280 $\mu\text{Gy day}^{-1}$ over the solar cycle. The standard deviation, typically 10% of the measured value, is due to variations in the Shuttle shielding experienced by the astronauts. For comparison, the average Mir cosmonaut (Commander and Flight Engineer) dose rate varied from 182 $\mu\text{Gy day}^{-1}$ to 397 $\mu\text{Gy day}^{-1}$ (2).

GALACTIC COSMIC RADIATION

Figure 3 shows the integral linear energy, y (\equiv ionization loss/mean detector chord length), spectra of GCR particles. A variation of a factor of ~ 2 in the flux is observed from solar minimum to solar maximum.

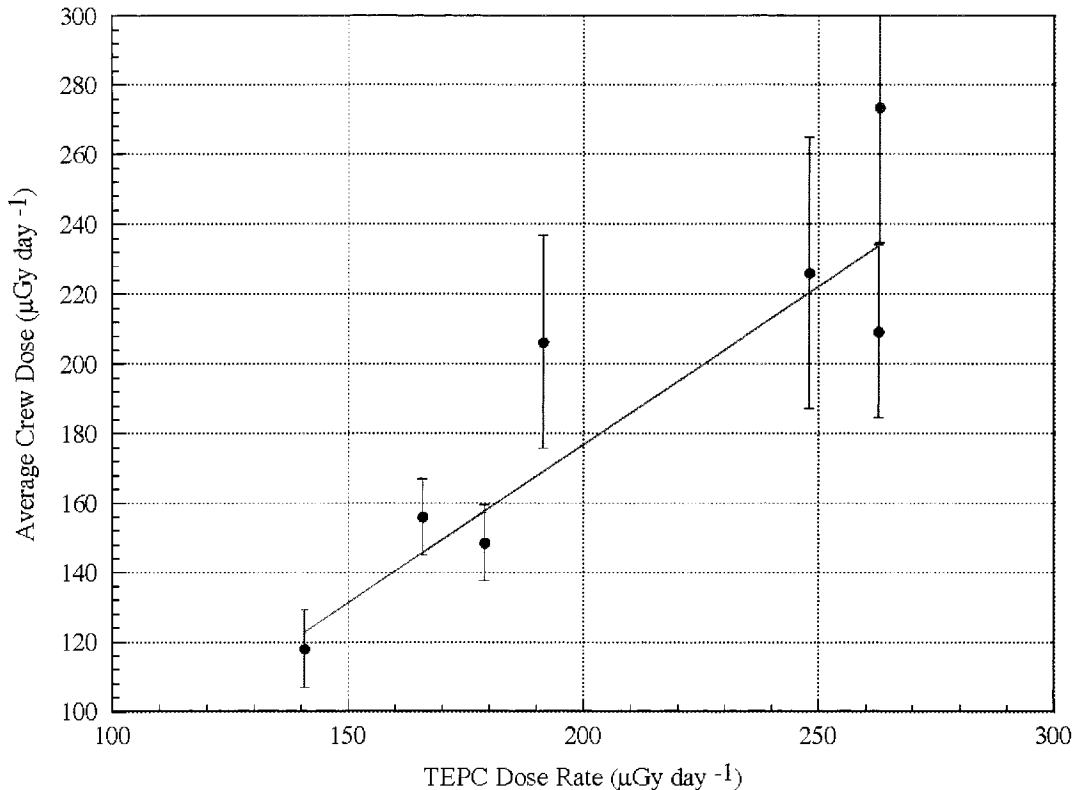


FIG. 2. A cross-plot of average dose rate measured by the TLD and the dose rate measured by the TEPC.

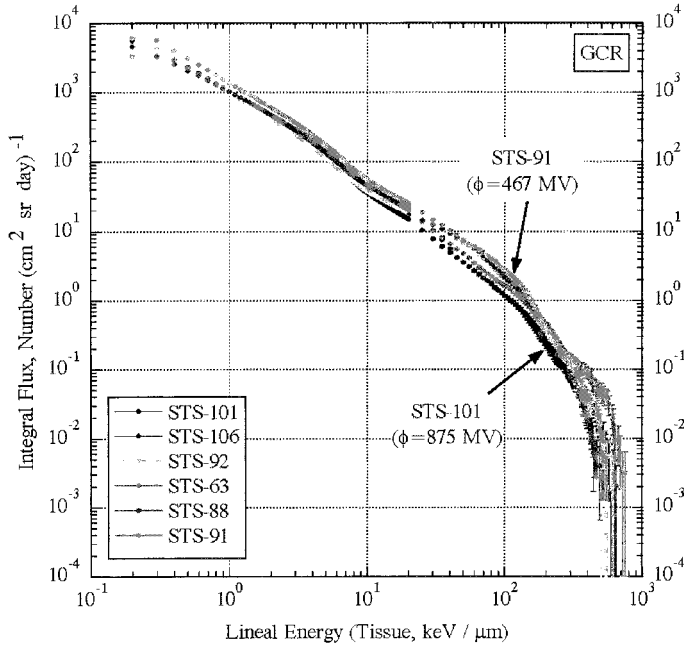


FIG. 3. Lineal energy spectra of GCR particles throughout the current solar cycle.

Figure 4 plots the measured dose rate, D_{GCR} , as a function of the deceleration potential, ϕ . The statistical uncertainty in the measurements is less than 1%, but uncertainties in detector calibration could be as much as 6% (5). The mean dose rate dropped by about 30% from solar minimum to solar maximum. The solid line is a least-squares fit: $(D_{\text{GCR}})^{-1} (\mu\text{Gy}^{-1} \text{ day}) = 9.6 \times 10^{-3} - 0.234 (\phi - 425)^{-1} + 4.94 (\phi - 425)^{-2}$. Badhwar and Cucinotta (9) showed that for a fixed solar modulation potential, the dose rate inside a reasonably well-shielded module is weakly dependent on moderate additional changes in the shielding distribution. A comparison of the RRMD-III (10) measured rate of $162 \mu\text{Gy day}^{-1}$ with the TEPC measured rate of $169 \mu\text{Gy day}^{-1}$ on STS-91 point in this direction. These STS-91 measured rates are 20% higher than the dose rate calculated using the HZETRN radiation transport code (11), the GCR environment model (9), the geomagnetic transmission function³ (12), and the TEPC shielding distribution. The average Mir GCR dose rates (2) are also plotted and, within the errors, show good agreement with the Shuttle data. The larger errors in the Mir data arise from the changes in its altitude that change the instantaneous geomagnetic cutoff. These results suggest that the quadratic fit given above can be used to predict the dose rate at locations inside the habitable Space Station modules to better than $\pm 10\%$, which is the largest deviation of points from the fitted line.

³ D. F. Smart and M. A. Shea, Description of the 5 Degree by 5 Degree Geomagnetic Cutoff Interpolation Method. Internal Report, Space Radiation Analysis Group, Johnson Space Center, Houston, 2000.

TRAPPED-BELT PARTICLES

Figure 5 shows the variation in the lineal energy spectra from solar minimum to solar maximum, including the variations due to the 30-km change in altitude. A factor of ~ 5 variation in flux due to both the altitude variation and the solar cycle variation can be expected on an ISS module. The RRMD-III measured a trapped dose rate of $271 \mu\text{Gy day}^{-1}$ on STS-91 compared to the TEPC-measured rate of $310 \mu\text{Gy day}^{-1}$. The 10% difference in dose rate is due to the differences in shielding distributions at the two locations. Model calculations using the radiation transport code (11), the orbit-averaged AP-8MIN solar minimum trapped spectrum,⁴ and the shielding distribution for the TEPC location gave a dose rate of $308 \mu\text{Gy day}^{-1}$.

Shuttle flights reach the ISS orbit in multiple altitude steps. The ISS altitude was raised during STS-101 and -106 and thus provided trapped-particle dose rates at differing altitudes. Pfitzer (13) pointed out that the trapped dose rate for 28.5° inclination Space Station Freedom could be organized as a function of atmospheric density. This was shown to be true for the 28.5° and 57° inclination Shuttle flights (3), which spanned two solar cycles, and also for the restricted Mir TEPC data (2). This was also shown using data from the TIROS spacecraft (14). Figure 6 is a plot of the trapped dose rates as a function of the atmospheric density, ρ . The density was calculated using the simplified Air Force Density model (13) and the actual Shuttle flight altitude crossing the SAA. There are clearly two groups of data. The lower solid line is a power-law fit: $D_{\text{trapped}} = (2.06 \pm 0.15) \times 10^{-8} \rho^{-(0.67 \pm 0.02)} \mu\text{Gy day}^{-1}$, with a χ^2 per degree of freedom, χ^2_{df} , of 0.8, the largest deviation of data from the fitted line being about 5%. A fit to the upper curve gives the power-law fit: $D_{\text{Trapped}} = (1.03 \pm 3.42) \times 10^{-10} \rho^{-(0.85 \pm 0.11)}$. The plotted line is 1.63 times the lower curve; that is, at the same atmospheric density, the dose rate can be 1.63 times higher because of the directional distribution of the trapped particles and the asymmetry of the Shuttle shielding distribution.

Using the AP-8MIN solar minimum trapped-belt model⁴ and the Mir TEPC shielding distribution function, we showed that the calculated dose-rate dependence on altitude was nearly identical to that calculated for the Shuttle shielding distribution. The agreement suggested that the Mir data should be in agreement with the Shuttle observations. The Mir data are plotted in Fig. 7. The χ^2_{df} of fitting the Shuttle TEPC distribution to the Mir data is 0.49, which is an excellent fit. The largest deviation was at the lowest density, and even here the Shuttle data fit the Mir data within one standard deviation. The errors in the Mir data are due to the diurnal variations (15). Thus the derived power law with atmospheric density that spans the entire expected ISS altitude range and solar conditions fits both the Shuttle data and the Mir data very well. As already shown using a less

⁴ D. Heynderickx, SPENVIS SPace ENVironment Information System, <http://www.spennis.oma.be/spennis>.

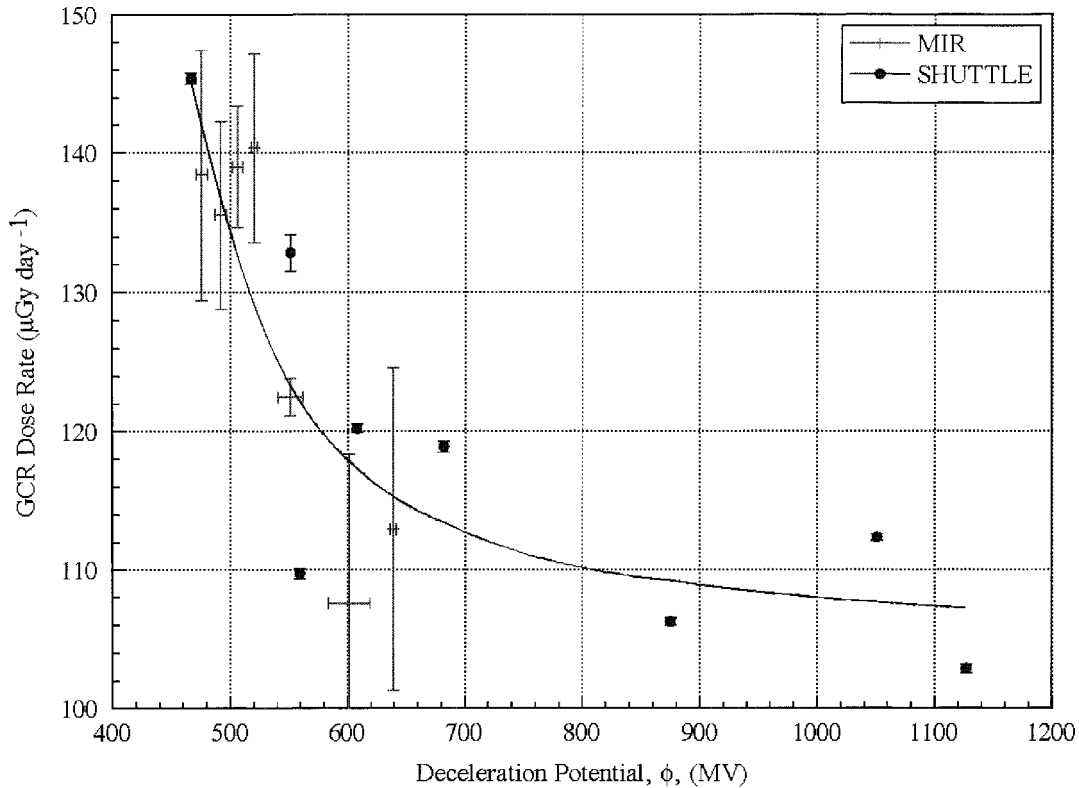


FIG. 4. GCR measured dose rates as a function of the deceleration potential.

accurate method, the TLD-100 data (3) also fit a power-law function with nearly the same indices at six other Shuttle locations.

Using the AP-8 solar-minimum trapped-belt spectra (14), the dose rate–altitude dependence at the M5005 shielding

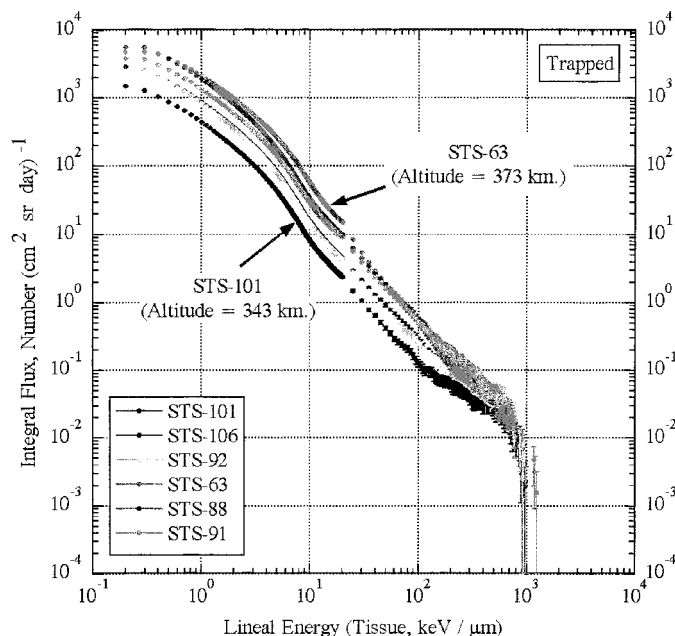


FIG. 5. Variation in the measured lineal energy spectra of trapped particles with solar activity.

location was calculated. The altitude dependence was converted to atmospheric density and normalized to the Shuttle data and is plotted in Fig. 7. Although it is not as good a fit as the power-law function given in Fig. 7, the normalized fit to the Shuttle data is accurate to $\sim 10\%$, except at the highest atmospheric density, where dose rates are very small. Thus the normalized fit can be used to predict dose rates at locations where the shielding distribution is known, and east–west effects are considered to be small.

The analysis of the 51.65° inclination Space Shuttle TEPC data and their consistency with the Mir observations and model calculations have provided fits for both trapped-particle radiation and galactic cosmic radiation that can be used to predict radiation dose rates to better than $\pm 15\%$ at any time in the solar cycle. The predictions of the trapped dose rate can be made correctly only if the altitude of the passage of the ISS through the SAA is known, information that should routinely be available.

CONCLUSIONS

An analysis of data acquired by TEPC instruments on Shuttle flights in the ISS 51.65° inclination orbit that span the current solar cycle from minimum to maximum, and the expected ISS altitude range, has shown the following: (1) A simple function of the solar deceleration potential describes the GCR dose rate throughout the solar cycle. It can be used to estimate the GCR dose rate to an accuracy

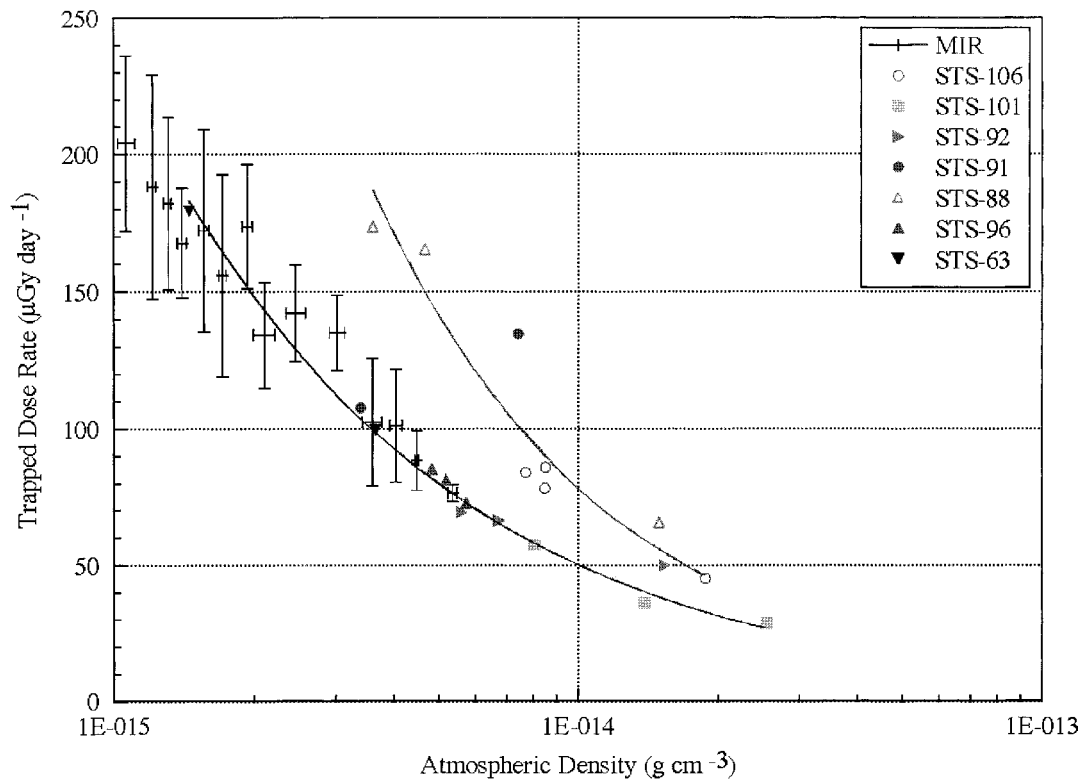


FIG. 6. Plot of trapped dose rate as a function of atmospheric density.

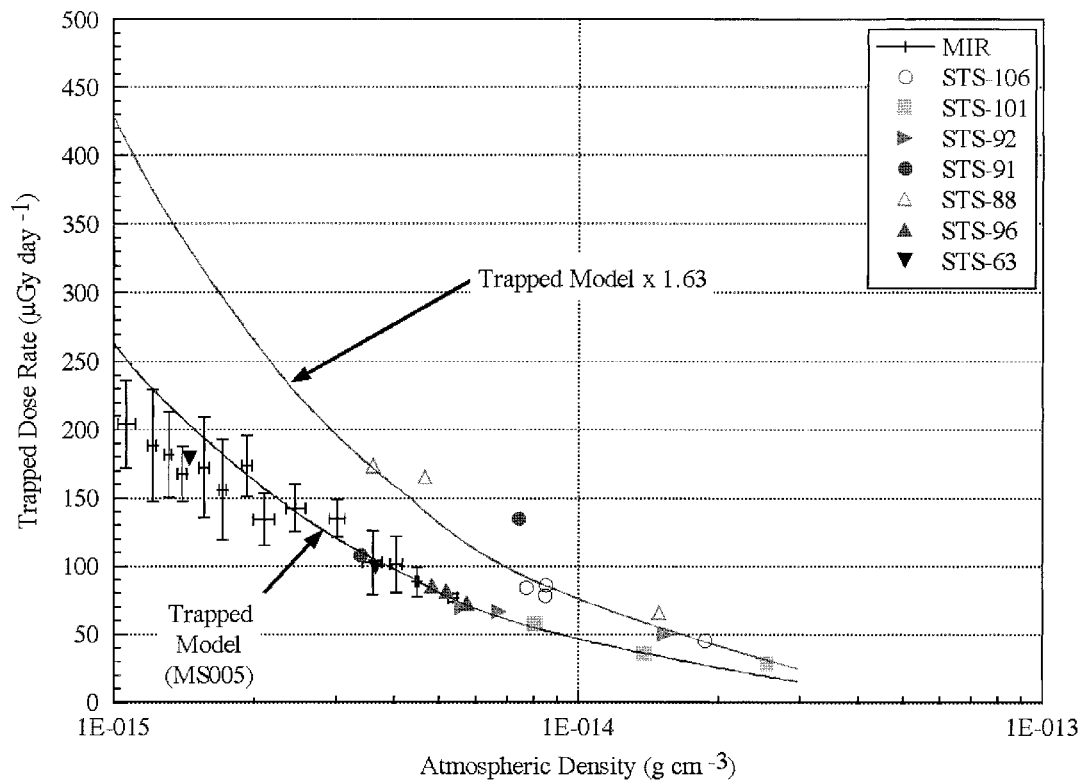


FIG. 7. Same data as in Fig. 6; the curves are calculated using scaled solar minimum model and shielding distribution.

of $\pm 10\%$. (2) The trapped-particle dose rate depends on the Shuttle orientation, which is consistent with earlier measurements. (3) Over the expected ISS altitude range and solar activity, the trapped-particle dose rate is shown to be a power-law function of the atmospheric density computed using the altitude of the SAA crossing, with a residual error of less than 5%. (4) This dose–density relationship can be derived (to a normalization factor) using the AP-8 trapped-belt model, but with somewhat lower accuracy. (5) Combining the error estimates of the GCR and SAA dose rates, the present results can be used to estimate the ISS dose rate to better than $\pm 15\%$ throughout the expected lifetime of the ISS. Solar energetic particles must be treated separately.

ACKNOWLEDGMENTS

Mr. Fadi Riman and Joel Flanders, Lockheed-Martin, Houston, provided considerable help in processing the flight data. Mr. Edward Semones, Lockheed-Martin Inc., provided the TLD measured Shuttle astronaut. Thanks are due to William Atwell, Boeing Inc., for the STS-63 correction.

Received: February 2, 2001; accepted: September 21, 2001

REFERENCES

1. V. M. Petrov, Overview on experience to date on human exposure to space radiation. *Adv. Space Radiat.* **14**, 397–408 (1994).
2. G. D. Badhwar, Radiation measurements in low Earth orbit: U.S. and Russian results. *Health Phys.* **79**, 507–514 (2000).
3. G. D. Badhwar, Radiation dose rates in Space Shuttle as a function of atmospheric density. *Radiat. Meas.* **30**, 401–414 (1999).
4. G. D. Badhwar, V. A. Shurshakov and V. V. Tsetlin, Solar modulation of dose rate onboard the MIR station. *IEEE Trans. Nucl. Sci.* **44**, 2529–2541 (1997).
5. G. D. Badhwar, F. A. Cucinotta, L. A. Braby and A. Konradi, Measurements on the Shuttle of the LET spectra of galactic cosmic radiation and comparison with radiation transport model. *Radiat. Res.* **139**, 344–351 (1994).
6. G. D. Badhwar, M. J. Golightly, A. Konradi, W. Atwell, J. W. Kern, B. Cash, E. V. Benton, A. L. Frank, D. Sanner and W. Schoner, In-flight radiation measurements on STS-60. *Radiat. Meas.* **26**, 17–34 (1996).
7. G. D. Badhwar, V. V. Kushin, Y. A. Akatov and V. A. Myltseva, Effects of trapped proton flux anisotropy on dose rates in low Earth orbit. *Radiat. Meas.* **30**, 415–426 (1999).
8. G. D. Badhwar and P. M. O'Neill, Galactic cosmic radiation model and its applications. *Adv. Space Res.* **17**, 7–17 (1996).
9. G. D. Badhwar and F. A. Cucinotta, A comparison of the depth dependence of dose and linear energy transfer spectra in aluminum and polyethylene. *Radiat. Res.* **153**, 1–8 (2000).
10. T. Doke, T. Hayashi, J. Kikuchi, T. Sakaguchi, K. Tersawa, E. Yoshihira, S. Nagaoka, T. Nakano and S. Takahashi, Measurements of LET-distribution, dose equivalent and quality factor with the RRMD-III on the Space Shuttle Missions STS-84, -89, and -91. *Radiat. Meas.* **33**, 373–388 (2001).
11. J. W. Wilson, F. F. Badavi, F. A. Cucinotta, J. L. Shinn and G. D. Badhwar, *HZETRN: Description of a Free-Space ion and Nucleon Transport and Shielding Computer Program*. NASA TP 3495, National Technical Information Service, Springfield, VA, 1995.
12. G. D. Badhwar, A. G. Troung, P. M. O'Neill and V. Choutko, Validation of galactic cosmic ray and geomagnetic transmission models. *Radiat. Meas.* **33**, 361–368 (2001).
13. K. A. Pfitzer, *Space Station Radiation Dose as a Function of Atmospheric Density*. MDSCC Report no. H5387, McDonnell Douglas Space System, Advanced Technology Center, Huntington Beach, CA, 1989.
14. S. L. Huston, G. A. Kuck and K. A. Pfitzer, Solar cycle variation of low-altitude trapped flux. *Adv. Space Res.* **21**, 1625–1634 (1998).
15. T. Dachev, J. V. Semkov, Y. N. Matviichuk, B. T. Tomav, R. T. Kaleva, V. M. Petrov, V. V. Shurshakov and Y. Ivanov, Inner magnetospheric variations after solar proton events. *Adv. Space Res.* **22**, 521–524 (1998).